



Article

Antioxidants Derived from Natural Products Reduce Radiative Damage in Cultured Retinal Glia to Prevent Oxidative Stress

Richard N. Cliver ¹, Natalia Castro ¹, Thais Russomano ² , Gaetano Lardieri ³ , Lindsay Quarrie ⁴, Helena van der Merwe ⁵ and Maribel Vazquez ^{1,*}

¹ Department of Biomedical Engineering, The State University of New Jersey, Rutgers University, 599 Taylor Road, BME-219, Piscataway, NJ 08854, USA; rnc54@scarletmail.rutgers.edu (R.N.C.); ngc42@scarletmail.rutgers.edu (N.C.)

² InnovaSpace UK, 88 Tideslea Path, London SE28 0LZ, UK; thais@innovaspace.org

³ Future Entheogenic Medicines, 44 Rome Street Suite 10, Newark, NJ 07105, USA; gaetanothcbd@gmail.com

⁴ Space Sciences Corp., 181A West Frontage Road, Lemitar, NM 87823, USA; lindsay@spacevitae.com

⁵ A-Plus-Consulting LLC, 211 Warren Street, Newark, NJ 07103, USA; helena@a-plus-consulting.com

* Correspondence: mv582@soe.rutgers.edu

Abstract: Retinal pathologies have been heavily studied in response to radiation and microgravity, including spaceflight-associated neuro-ocular syndrome (SANS), which is commonly developed in space flight. SANS has been characterized in clinical studies of astronauts returning to Earth and includes a range of symptoms, such as globe flattening, optic-disc edema, retinal folds, and retinal ischemia. In cases of retinal insult, Müller glia (MG) cells respond via neuroprotective gliotic responses that may become destructive to produce glial scarring and vision loss over time. Retinal pathology is further impacted by the production of excessive reactive oxygen species (ROS) that stimulate retinal inflammation and furthers the gliosis of MG. Neuroprotectants derived from natural products (NPs) able to scavenge excess ROS and mitigate long-term, gliotic responses have garnered recent interest, especially among mature and aging adults. The natural antioxidants aloin and ginkgolide A flavonoids, derived from *Aloe vera* and *Ginkgo biloba* species, respectively, have been of particular interest due to their recent use in other nervous-system studies. The current study examined MG behaviors in response to different doses of aloin and ginkgolide A over time by measuring changes in morphology, survival, and ROS production within microscale assays. The study was further enhanced by using galactic cosmic rays (GCR) at the Brookhaven NASA Space Radiation Laboratory to simulate ionizing radiation in low- and high-radiation parameters. Changes in the survival and ROS production of radiation-treated MG were then measured in response to varying dosage of NPs. Our study used *in vitro* systems to evaluate the potential of NPs to reduce oxidative stress in the retina, highlighting the underexplored interplay between NP antioxidants and MG endogenous responses both in space and terrestrially.

Keywords: Müller glia; aloin; ginkgolide A; galactic cosmic rays; ionizing radiation; oxidation-reduction; reactive-oxygen species (ROS)



Citation: Cliver, R.N.; Castro, N.; Russomano, T.; Lardieri, G.; Quarrie, L.; van der Merwe, H.; Vazquez, M. Antioxidants Derived from Natural Products Reduce Radiative Damage in Cultured Retinal Glia to Prevent Oxidative Stress. *Neuroglia* **2022**, *3*, 84–98. <https://doi.org/10.3390/neuroglia3030006>

Academic Editor: James St John

Received: 24 May 2022

Accepted: 15 July 2022

Published: 20 July 2022

Publisher's Note: MDPI stays neutral with regard to jurisdictional claims in published maps and institutional affiliations.



Copyright: © 2022 by the authors. Licensee MDPI, Basel, Switzerland. This article is an open access article distributed under the terms and conditions of the Creative Commons Attribution (CC BY) license (<https://creativecommons.org/licenses/by/4.0/>).

1. Introduction

The National Aeronautics and Space Administration (NASA) has recently documented the development of ocular pathologies in response to the microgravity and ionizing radiation of space, called spaceflight-associated neuro-ocular syndrome (SANS) [1]. While SANS is believed to be primarily microgravity-driven, how these ocular manifestations may occur as byproducts of radiation exposure [1–3] remains unknown. Ionizing radiation is known to induce injuries in biological tissue, including cerebro-ophthalmic injuries within the eye and retina, at high and low doses of radiation [4,5]. Damage to photoreceptors has been reported for up to two years post-irradiation in high energy ^{56}Fe (iron ion) studies [6,7]. These ^{56}Fe high energy nuclei are difficult to defend against, fragmenting in contact with

shielding materials and depositing high-energy particles within the biological tissues of astronauts. Projects have also shown that high doses of 56Fe can cause cellular death and retinal microlesions for months following a retinal injury [8,9]. Importantly, neural studies of astronauts have reported that low-dosage radiation can affect brain-retinal-barrier functions (BRB), causing neovascular remodeling and increased retinal-cell apoptosis [3]. These issues have received increased significance with the higher frequency and duration of commercial air travel [10] and, most recently, with the advent of space tourism [11]. How ionizing radiation influences reduction-oxidation processes within the retina to result in degeneration and vision loss is unknown.

Reduction-oxidation, or redox reactions, provide the main source of energy for essential cellular functions in the vertebrate retina [12–14]. The retina is a highly cellular and multi-laminated tissue that enables phototransduction of light to form images of objects in the brain, as shown in Figure 1. The human retina connects the eye directly to the visual cortex through the optic nerve and contains six different neuronal cell lineages and one primary neuroglia, called Müller glia (MG).

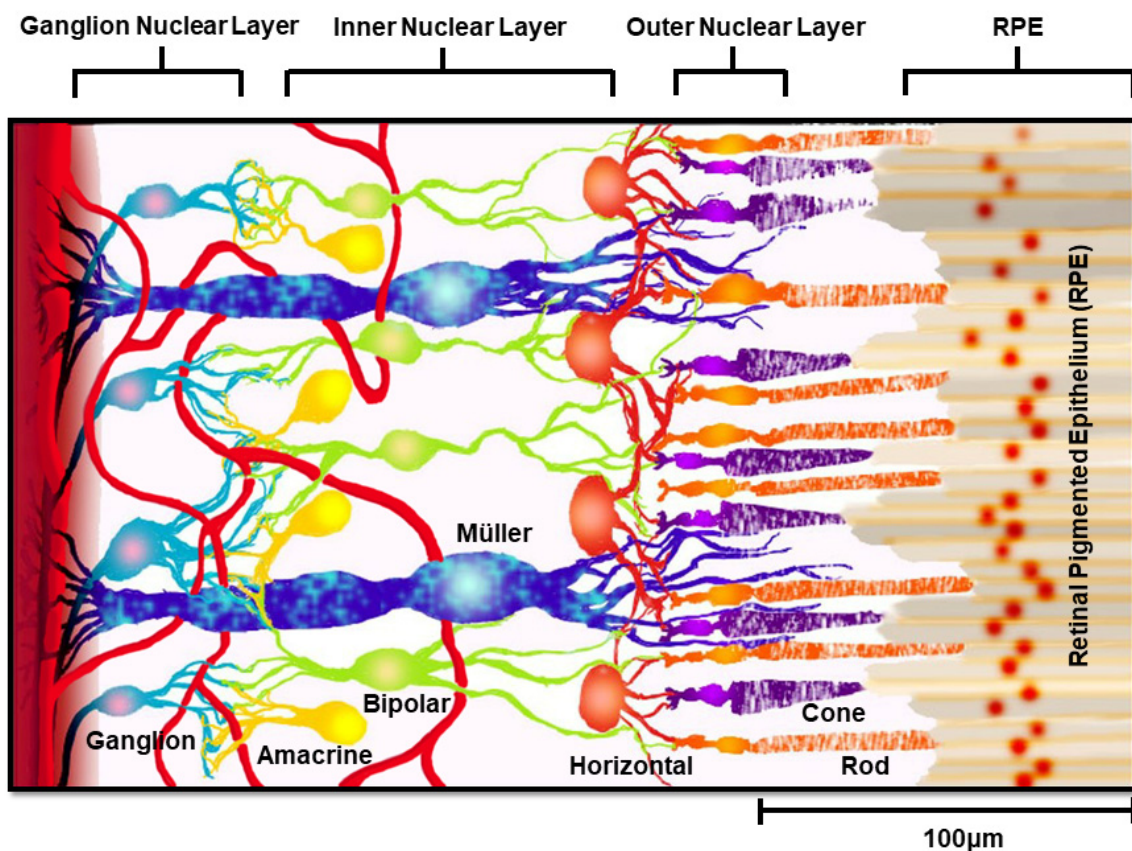


Figure 1. Layered schematic of the retina. A rendering of the human retina showing synaptic connections between Müller glia (blue) and retinal ganglion cells (teal), amacrine cells (yellow), bipolar cells (green), horizontal cells (orange), and photoreceptors (rods: orange; cones: purple).

The visual system's daily exposure to light increases retinal-oxygen consumption, to elevate its tissue levels of free radicals, including reactive nitrogen, iron, and oxygen species [15]. Reactive-oxygen species (ROS) are intracellular signaling molecules that regulate neuronal function and vascular reactivity [16], but with excess production that can modify or impair molecular-retinal functions, stimulate apoptosis, and inflammatory responses [17]. ROS production due to elevated retinal metabolism is well-known to contribute to neurodegenerative disorders, such as SANS, age-related macular degeneration (AMD), and diabetic retinopathy (DR), among others [18–20]. As a result, rising adult inter-

est in eye-health supplements has been reflected by exponential growth in the nutraceutical market [21–24], shown in Figure 2.

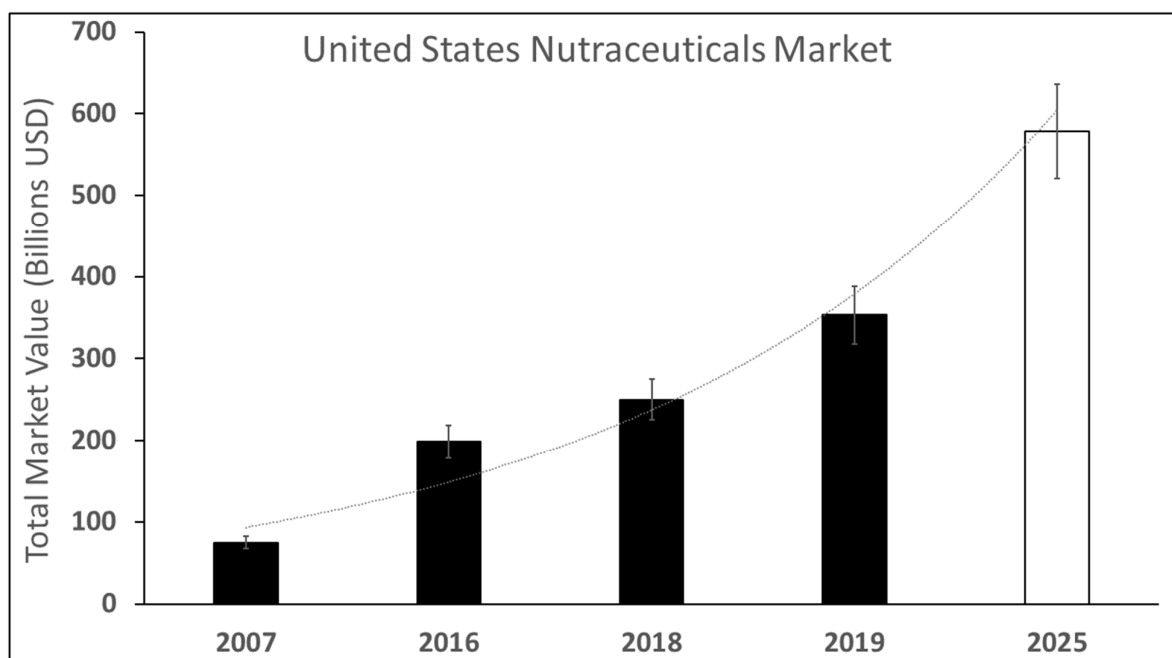


Figure 2. Estimated and projected growth of the nutraceuticals market in the United States from 2007–2025. The total market value of the nutraceuticals market from 2007–2025. Dark bars represent measured expenditures of total market values in billions of USD, while the white bar denotes projections in upcoming years.

While the underlying mechanisms of retinal degeneration from SANS and other degenerative pathologies remain only partially understood [25], excessive ROS are major cytotoxic factors that promote retinal insult via oxidative stress, resulting in progressive vision loss [26,27]. MG are mechano-sensing cells that control retinal metabolism [28,29], regulate permeability of the blood retinal barrier (BRB) [30], and respond to insults via gliosis (reviewed in [31,32]), a series of endogenous-repair responses that protect neurons and isolate damaged cells as needed. Significantly, oxidative stress not only lessens MG neuroprotective abilities but also promotes chronic, neurodestructive MG responses. Here, MG respond to long-term injury via migration and proliferation that can displace adjacent neurons, disrupt synaptic networks, and lead to glial scarring [32,33]. Moreover, elevated ROS stimulates pathological MG activity, which includes increased secretion of the inflammatory cytokine tumor necrosis factor alpha (TNF- α) [34], vasodilation via nitric oxide [35], oxidation of the glutamine synthetase protein [36], and oxidative stress via accumulation of advanced glycation end products (AGEs), recently shown to alter BRB permeability [37]. As a result, antioxidant substances from natural products (NPs) that scavenge excess ROS production and protect against oxidative stress have become therapeutic targets as neuroprotectants against eye-related dysfunction and retinal disease [38]. The antioxidant and radical-scavenging properties of aloin, an anthraquinone-C-glycoside found in the Aloe species, and ginkgolide A of the Ginkgo biloba species [39,40], have been recently used to reduce cell-membrane lipid peroxidation and subsequent damage to lipid membranes in retinal neurons [41]. However, few projects have examined the effects of any of these NPs on MG behaviors, despite the known reparative properties of these retinal neuroglia [39,42,43].

The current project used microscale, *in vitro* systems to examine the behaviors of reactive MG with and without dosages of aloin (A) and ginkgolide A (G) in response to galactic cosmic rays (GCR), which simulate solar-ionizing radiation in low- and high-

radiation parameters. Results of our study illustrate the ability of these NP antioxidants to promote MG survival, induce changes in morphology, and reduce production of excess ROS with varying cumulative doses of GCR. These data highlight the importance of using antioxidants to examine MG behaviors against oxidative damage from SANS and other retinal-degenerative disorders as well as the translational significance of NP formulations that reduce ROS production in aging retina.

2. Materials and Methods

2.1. Cell Culture

Müller glia (MG) were modeled using an immortalized cell line (rMC-1; Kerafast, ENW001), immortalized by transfecting primary Müller cell cultures from adult-rat retinas with a viral oncogene [44], and were thawed from aliquots stored in nitrogen tanks, before being plated onto sterile, tissue culture flasks, and cultured using sterile Dulbecco's modified Eagle medium (DMEM; ATCC, Cat. No. 30–2002) containing 10% fetal bovine serum (Thermo Fisher Scientific, Waltham, MA, USA; Cat. No. 26140) and 1% penicillin-streptomycin (Gibco, New York, NY, USA, Cat. No. 15070063). All cells were cultured at 37 °C, 95% humidity, and 5% CO₂ and passaged at 80%–90% confluence. To dislodge cells from the flask, cultures were rinsed once with Dulbecco's Phosphate Buffered Saline (DPBS; VWR, 21-031-CV) then incubated in Accutase (ICT, Inc., San Diego, CA, USA, Cat. No. AT104-500) for 10 min at 37 °C and centrifuged at 1500 rpm for 3 min. Cell medium was replaced every 2 days, and cultures were allowed to reach 80–90% confluence before harvesting for testing. rMC-1 cells have been used to model the behaviors of MG by our group [45] and others [44,46,47]. Our current study continued to use these models to maintain appropriate comparisons across studies.

2.2. Reagents

MG cultures were examined in response to exogenous 10 µg/mL, 50 µg/mL, 100 µg/mL, 250 µg/mL, and 500 µg/mL concentrations of aloin (A: Thermo Fisher Scientific, Cat. No. AAJ62153MC); 0.5 µg/mL, 1 µg/mL, 2.5 µg/mL, 5 µg/mL, and 10 µg/mL concentrations of ginkgolide A (G: Thermo Fisher Scientific, Cat. No. 11-101-3216). A summary of the concentration used and their denotations in experiments are listed in Table 1.

Table 1. Survival rates of Müller glia (MG) in response to exogenous concentrations of antioxidant solutions. Survival rates of Müller glia (MG) measured when cultured in different antioxidant solutions of aloin (A) and ginkgolide A (G) for 72 h. Statistical significance is denoted with an asterisk (*) for $p < 0.05$ and with a triple asterisk (***) for $p < 0.001$.

Aloin	Control	10 µg/mL	50 µg/mL	100 µg/mL	250 µg/mL	500 µg/mL
72 h	97.0 ± 5.6%	94.4 ± 3.7%	93.4 ± 4.5%	90.5 ± 3.5%*	73.5 ± 13.0% ***	63.3 ± 10.0% ***
Ginkgolide A	Control	0.5 µg/mL	1 µg/mL	2.5 µg/mL	5 µg/mL	10 µg/mL
72 h	99.3 ± 0.2%	99.5 ± 0.5%	98.7 ± 0.3%*	96.3 ± 1.6%*	95.8 ± 3.7%	93.8 ± 2.7%*

2.3. Measurement of Cell Survival, Morphology, Proliferation, and GOS

Cells were seeded at 20,000 cells per mL in 24-well plates (Corning, New York, NY, USA, Cat. No. 353047). Representative cell groups were analyzed at 0 h (immediately upon seeding), 24 h, 48 h, and 72 h. The morphology of MG was evaluated via the cell-shape index (CSI), as accomplished previously by our group [48,49], using the dimensionless parameter to quantify the roundness of a cell and as per Equation (1):

$$\text{CSI} = (4\pi A_s)/P^2 \quad (1)$$

where AS is the cell surface area (μm^2), and P (μm) is the perimeter of the cell. The value of the CSI ranges from 0 to 1, where values close to one represent a perfectly rounded cell, and values approaching 0 denote a purely bipolar and elongated cell [48].

Proliferation and survival were calculated using a LIVE/DEAD Viability/Cytotoxicity Kit for mammalian cells (Thermo Fisher Scientific, Cat. No. L3224). The LIVE/DEAD assay reagent treated cells with calcein-AM and ethidium homodimer-1 administered for 30 min at room temperature ($T = 25^\circ\text{C}$), which were then immediately imaged. Survival is defined in Equation (2):

$$\text{Survival} = (L - D)/L \cdot 100\% \quad (2)$$

where L (Live) is the average of calcein-AM stained cells across three wells in triplicate, and D (Dead) is the average of ethidium homodimer-1-stained cells across 3 wells in triplicate. This number is then expressed as a percent between 0% and 100%. Proliferation was defined as the number of Live cells in representative well images averaged over all time points and normalized to the 24-well-plate area ($A = 2 \mu\text{m}^2$). The survival difference is computed in Table 2 as the Post-Treatment Survival % subtracted from the Pre-Treatment Survival %.

Table 2. Survival rates of Müller glia (MG) in response to exogenous concentrations of antioxidant solutions. Survival rates of Müller glia (MG) measured when cultured in different antioxidant solutions of aloin (A) and ginkgolide A (G) for 30 min and 6 h post irradiation. Survival difference computed as the (Pre-Treatment Survival—Post-Treatment Survival).

Pre-Treatment Survival		Post-Treatment Survival		(Pre – Post) Survival Difference
30 min				
Aloin Control	92.9%	Aloin Control	92.9%	0.0%
Aloin 50 $\mu\text{g}/\text{mL}$	92.2%	Aloin 50 $\mu\text{g}/\text{mL}$	92.1%	0.1%
Aloin 100 $\mu\text{g}/\text{mL}$	94.6%	Aloin 100 $\mu\text{g}/\text{mL}$	93.3%	1.3%
Ginkgolide A Control	95.1%	Ginkgolide A Control	94.1%	1.0%
Ginkgolide A 1 $\mu\text{g}/\text{mL}$	95.5%	Ginkgolide A 1 $\mu\text{g}/\text{mL}$	94.7%	0.8%
Ginkgolide A 2.5 $\mu\text{g}/\text{mL}$	93.2%	Ginkgolide A 2.5 $\mu\text{g}/\text{mL}$	95.1%	-1.9%
6 h				
Aloin Control	92.7%	Aloin Control	91.1%	1.6%
Aloin 50 $\mu\text{g}/\text{mL}$	91.3%	Aloin 50 $\mu\text{g}/\text{mL}$	95.8%	-4.5%
Aloin 100 $\mu\text{g}/\text{mL}$	94.7%	Aloin 100 $\mu\text{g}/\text{mL}$	90.3%	4.4%
Ginkgolide A Control	91.3%	Ginkgolide A Control	94.2%	-2.9%
Ginkgolide A 1 $\mu\text{g}/\text{mL}$	91.9%	Ginkgolide A 1 $\mu\text{g}/\text{mL}$	94.8%	-2.9%
Ginkgolide A 2.5 $\mu\text{g}/\text{mL}$	85.2%	Ginkgolide A 2.5 $\mu\text{g}/\text{mL}$	95.7%	-10.5%

Reactive-oxygen species (ROS) were calculated using CM-H2DCFDA kit (Thermo Fisher Scientific, Cat. No. C6827) to measure general oxidative stress (GOS) in MG. At the time points of $t = 0, 24, 48$, and 72 h , the GOS stain was administered for 30 min at 37°C , 95% humidity, and 5% CO_2 at a concentration of 30 μM [50]. Following incubation, the loading buffer was washed off with pre-warmed PBS (37°C) and cells were immediately imaged. GOS fold intensity was calculated using a parameter called the Corrected Total Cell Fluorescence (CTCF), defined in Equation (3):

$$\text{CTCF} = \text{ID} - (A_s \cdot \mu_B) \quad (3)$$

where ID is the Integrated Density calculated using optical software (Image J, National Institutes of Health, Boston, MA, USA), AS is the cell surface area (μm^2), and μ_B is the average of three background-intensity readings.

Cell groups were separated by “Pre-Treatment” and “Post-Treatment” conditions, which describe treatment with antioxidant solutions at 24 h before irradiation (Pre-Treatment) and immediately after irradiation (Post-Treatment).

2.4. Galactic Cosmic Rays (GCR)

The Galactic Cosmic Radiation (GCR) Simulator at the NASA Space Radiation Laboratory (NSRL) at Brookhaven National Laboratory was used to conduct the experiments [51]. A five-ion profile was chosen consisting of hydrogen protons at 1000 and 250 MeV ($Z = 1$), silicon at 600 MeV/n ($Z = 14$), helium at 250 MeV/n ($Z = 2$), oxygen at 350 MeV/n ($Z = 8$), and iron at 600 MeV/n ($Z = 26$). Hydrogen of 1000 MeV consisted of 35% of the total irradiation, silicone consisted of 1% of the total irradiation, helium consisted of 18% of the total irradiation, oxygen consisted of 6% of the total irradiation, iron consisted of 1% of the total irradiation, and hydrogen of 250 MeV consisted of 39% of the total irradiation. The total dose of ion species was 67 cGy delivered over 87.81 min, which is equivalent to a cumulative dose of a round trip to Mars. Additionally, a $10 \times 10 \text{ cm}^2$ beam delivered 300 MeV/n of iron to additional 12-well plates for a high-dosage, high-irradiation-rate iron bombardment. The cell subjected to this iron bombardment received 746.3% of the original 5 ion species GCR. A dose of 500 cGy was delivered over 8.9 min for a total dose rate of 57.4059 cGy/min, as shown in Figure 3.

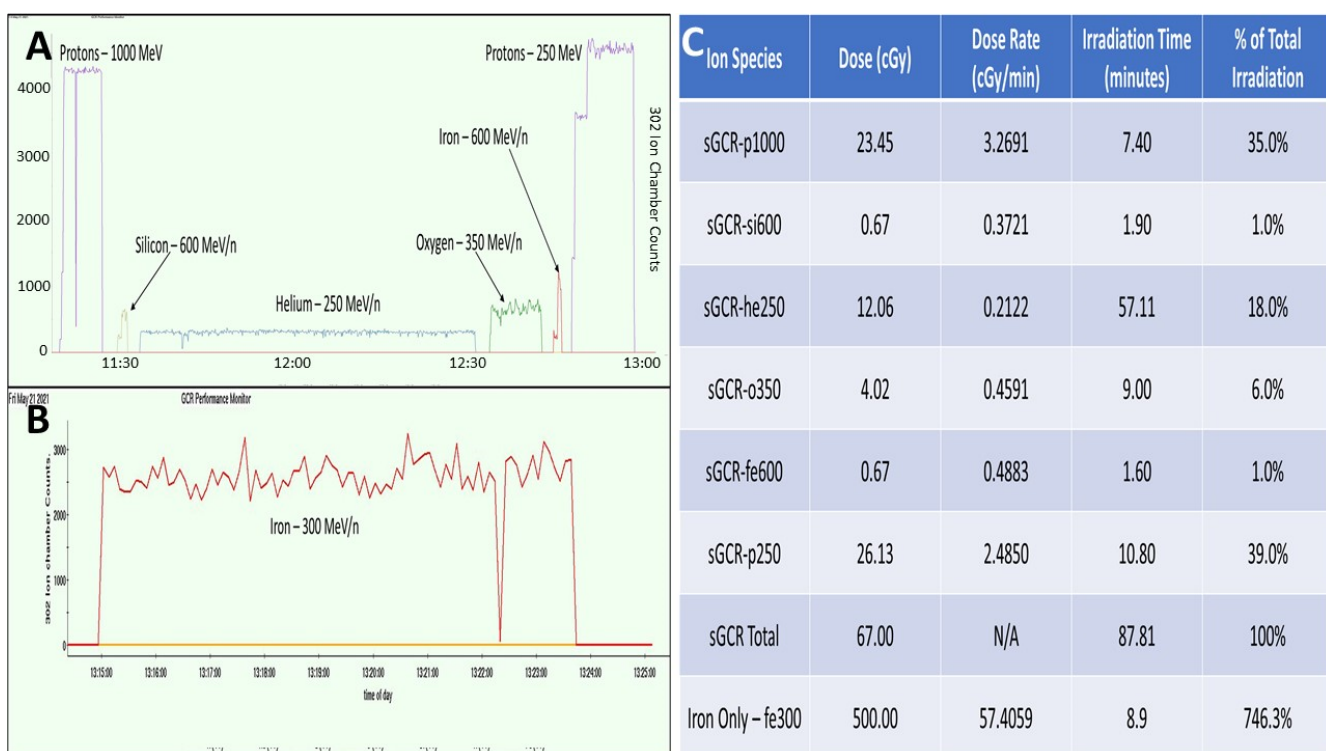


Figure 3. Methodology of NASA irradiation studies and use of galactic cosmic rays (GCR) in study of Müller glia (MG). (A) Graphical depiction of the GCR 5-ion study performed for irradiation values equivalent to a round trip to Mars (67 centiGray (cGy)). (B) Graphical depiction of the GCR iron-only study performed for high-irradiation conditions of 500 centiGray (cGy). (C) Graphical depictions represented numerically, split by Ion Species, Dose, Dose Rate, Irradiation Time, and % of Total Irradiation.

2.5. Imaging and Analyses

An inverted epi-fluorescence microscope (Leica DMi8) was used to observe cell behavior over time and to perform optical analyses with a cooled CCD camera (DFC7000 GT, Leica Microsystems, Wetzlar, Germany) using a $20\times$ magnification (DMi8 Leica Mi-

crosystems Inc., Buffalo Grove, IL, USA). An insertable frame for the microscope stage (H301-K-FRAME, Leica Microsystems) was used to hold the 24-well plates, with attachment (24MW, OKOLAB, Pozzuoli, Italy). Intensity values (16-bit scale: 0–65535) were measured using ImageJ (National Institutes of Health, Boston, MA, USA), as accomplished previously by our group [48]. An inverted epi-fluorescence microscope (Axiovert 200 M) was used to observe cell behavior post-irradiation at Brookhaven’s NSRL facility (Brookhaven National Laboratory, Upton, NY, USA).

2.6. Statistical Analyses

One-Way ANOVA was used to analyze statistical significance among all experimental groups. Each data set was gathered from a minimum of $n = 35$ cells per well, in triplicate. Mean values from a pilot study were used to compute an 80% power analysis using $n = 35$ cells per well, in triplicate. Microsoft Excel’s Data Analysis Toolbox was used for One-Way ANOVA testing and data analysis. Normality was confirmed through the use of the Shapiro–Wilk test, performed though the use of Graphpad Prism. Values are reported using standard error of the mean. Statistical significance of $p < 0.05$ is denoted with an asterisk (*), $p < 0.01$ is denoted with a double asterisk (**), and $p < 0.001$ is denoted with a triple asterisk (***)�.

3. Results

3.1. Changes in Müller Glia Morphology and Proliferation in Antioxidant Solutions

Differences in Müller glia (MG) morphology and proliferation rates were examined over 72 h, when cultured in antioxidant solutions of aloin (A: 10–500 μ g/mL) and ginkgolide A (G: 0.5–10 μ g/mL). MG in the control solution (C: DMEM only) exhibited increasingly elongated morphology over time, with measured values of the cell-shape index (CSI) decreasing from ${}^C\text{CSI}0 = 0.862 \pm 0.002$ to ${}^C\text{CSI}72 = 0.319 \pm 0.003$ over 72 h, as shown in Figure 4. These values were consistent for all control solutions across all experimental groups.

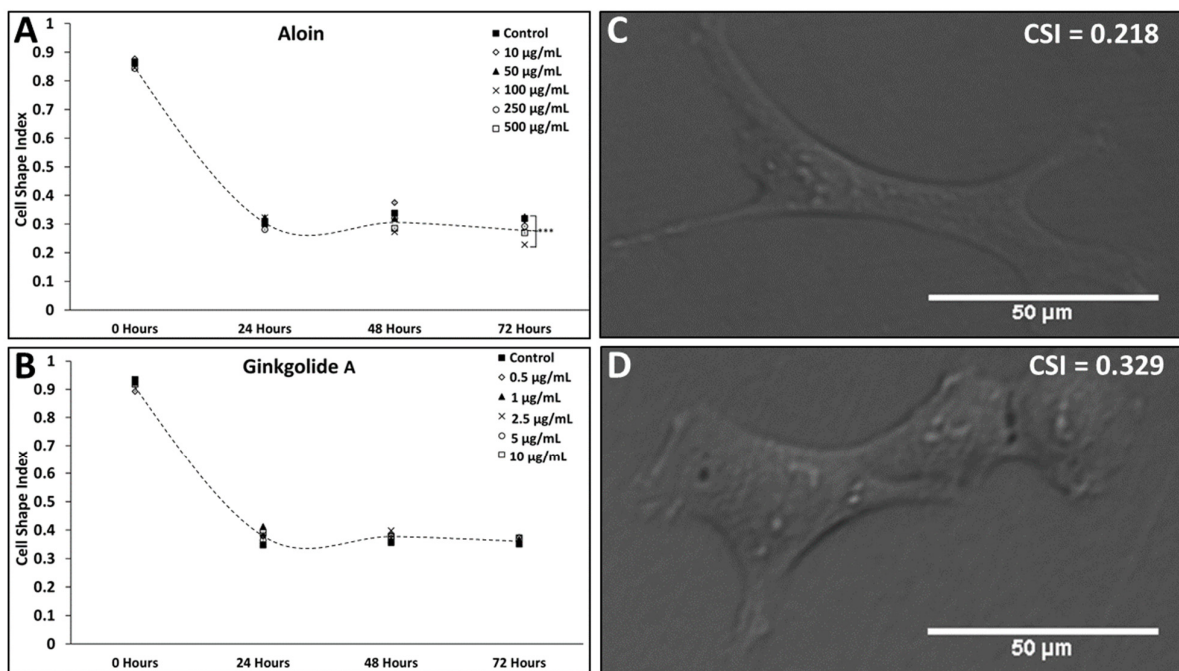


Figure 4. Changes in Müller glia (MG) morphology over time in response to exogenous concentrations of aloin (A) and ginkgolide A (G). Differences in the morphology of Müller glia (MG) cells cultured over time in different antioxidant solutions as represented via cell-shape index (CSI). Values of MG morphology measured in titrated solutions of (A) 10, 50, 100, 250, and 500 μ g/mL of aloin (suspended

in DMEM); (**B**) titrated solutions of 0.5, 1, 2.5, 5, and 10 $\mu\text{g}/\text{mL}$ of ginkgolide A (suspended in DMEM). Dashed curves through each plot denote changes in CSI over time for the control condition (DMEM only). Representative images of MG after 72 h of culture in (**C**) 100 $\mu\text{g}/\text{mL}$ of aloin (suspended in DMEM); (**D**) 1 $\mu\text{g}/\text{mL}$ of ginkgolide A (suspended in DMEM). Scale bar = 50 μm .

CSI values of MG cultured in extracellular solutions of aloin (A) followed a decreasing trend, with values of CSI ranging from $A^{-1}\text{CSI}24 = 0.877 \pm 0.001$ ($p > 0.05$ against the control) to $A^{-5}\text{CSI}72 = 0.269 \pm 0.003$ ($p > 0.05$ against control) for the concentrations listed. Notably, cells cultured in 100 $\mu\text{g}/\text{mL}$ (Concentration A-3) of aloin exhibited the most significant elongation over the control at 72 h with $A^{-3}\text{CSI}72 = 0.228 \pm 0.002$ ($p < 0.001$) (Figure 4A). By contrast, MG cultured in extracellular solutions of Ginkgolide A (G) exhibited no significant changes in cell morphology across all concentrations, with CSI values approaching that of the control at every time point (Figure 4B).

3.2. Changes in Cell Survival within Extracellular Solutions of Antioxidants

The survival rates, S , of MG cultured within different concentrations of exogenous antioxidants were measured over 72 h, as shown in Table 1. Aloin and ginkgolide A have been studied pre-radiation to quantify the survival rates of glial cells exposed to antioxidants under normal cell-culture conditions. The naming procedure used for aloin and ginkgolide A studies can be found in Figure S1. MG viability was measured using Equation (2) and compared across all time points $t = 0\text{ h}$ to $t = 72\text{ h}$. MG grown within aloin solutions exhibited a survival range between $A^{-1}S72 = 94.4\% \pm 3.70\%$ ($p > 0.05$) and $A^{-5}S72 = 63.3\% \pm 10.0\%$ ($p < 0.001$) over time. MG viability remained statistically insignificant against the control for all concentrations through $t = 48\text{ h}$ and remained above 97% viability. However, MG cultured within higher concentrations of 250 $\mu\text{g}/\text{mL}$ (concentration A-4) and 500 $\mu\text{g}/\text{mL}$ (concentration A-5) exhibited significantly decreasing survival at $t = 72\text{ h}$, with $A^{-4}S72 = 73.5\% \pm 13.0\%$ ($p < 0.001$) and $A^{-5}S72 = 63.3\% \pm 10.0\%$ ($p < 0.001$) (Table 1).

The changes in MG survival when cultured with different concentrations of ginkgolide A (G) were not significant against the control at $t = 48\text{ h}$, but exhibited significantly lower survival at $t = 72\text{ h}$. As seen, MG cultured in the highest concentration of 10 $\mu\text{g}/\text{mL}$ (concentration G-5) exhibited the lowest survival of $G^{-5}S72 = 93.8\% \pm 2.68\%$ ($p < 0.05$) (Table 2).

3.3. Changes in Oxidative Stress of Müller Glia within Extracellular Solutions

The oxidative stress expressed by MG in response to exogenous antioxidant solutions was measured via its production of reactive-oxygen species (ROS). MG levels of ROS varied significantly across antioxidant groups, as per Figure 6A,B. Timepoints taken in the $t = 0\text{ h}$ control group were normalized to a value of 1 for all studies, and all ANOVA testing was performed to each timepoint's control, respectively. The average value of ROS for the control conditions for all time points was $C\text{ROS}0-72 = 1.09 \pm 0.05$. As shown, MG cultured in aloin solutions of 100 $\mu\text{g}/\text{mL}$ (concentration A-3), and 250 $\mu\text{g}/\text{mL}$ (concentration A-4) exhibited significantly lower intensity at 0 h and slowly increased to the levels of the normalized control within 72 h. ROS generated by MG cultured within 10 $\mu\text{g}/\text{mL}$ (concentration A-1) and 100 $\mu\text{g}/\text{mL}$ (concentration A-3) of aloin were significantly greater at 72 h with values of $A^{-1}\text{ROS}72 = 2.19 \pm 0.47$ ($p < 0.01$) and $A^{-3}\text{ROS}72 = 1.74 \pm 0.26$ ($p < 0.05$). MG cultured within ginkgolide A (G) solutions produced highly significant changes in ROS at $t = 0\text{ h}$ but decreased to approach those of the control at 72 h with $G^{-1}\text{ROS}72 = 1.27 \pm 0.25$ ($p < 0.01$) as significantly higher than the control.

3.4. Changes in Survival and Oxidative Stress of Müller Glia Post-GCR

The survival rates, S , of MG cultured within different concentrations of exogenous antioxidants were measured over 6 h post irradiation, as shown in Table 2. MG viability was measured using Equation (2) and compared across the time points 30 min and 6 h.

Groups were separated by “Pre-Treatment” and “Post-Treatment”. This describes treatment with antioxidant solutions at 24 h before irradiation (Pre-Treatment) and immediately after irradiation (Post-Treatment). The oxidative stress expressed by MG post-radiation was measured via the production of reactive-oxygen species (ROS). MG levels of ROS varied significantly across antioxidant groups, as per Figure 5A,B. Aloin 100 µg/mL (A-3) showed a highly significant decrease in ROS at the 30 min time point for both the pre- and post-treatment groups. This difference was seen to be $^{Pre-A-3}ROS30 = 0.65 \pm 0.21$ ($p < 0.001$) and $^{Post-A-3}ROS30 = 0.44 \pm 0.19$ ($p < 0.001$), against the controls of $^{Pre-C}ROS30 = 1.00 \pm 0.22$ and $^{Post-C}ROS30 = 0.98 \pm 0.22$, respectively. This significance decreased to that of the control by 6 h. Ginkgolide A seemed to have an opposite effect in Figure 5B, with values differing little from the control at 30 min and significance among the Post-Treatment group at 6 h. $^{Post-G-2}ROS6 = 1.96 \pm 0.22$ ($p < 0.05$) and $^{Post-G-3}ROS6 = 2.43 \pm 0.25$ ($p < 0.001$), against the control of $^{Post-C}ROS6 = 1.35 \pm 0.21$.

MG cultured for testing in the high-dosage iron-only study underwent a shorter irradiation time and a far greater dose rate, as seen in Figure 7C. MG were studied under the post-treatment condition at 30 min for survival and ROS. Aloin treatment showed no significant effect at the 30 min time point, however, ginkgolide A treatment provided significance at 30 min. $^{Post-G-3}ROS30 = 0.76 \pm 0.20$ ($p < 0.05$) compared to the control $^{Post-C}ROS30 = 1.00 \pm 0.22$.

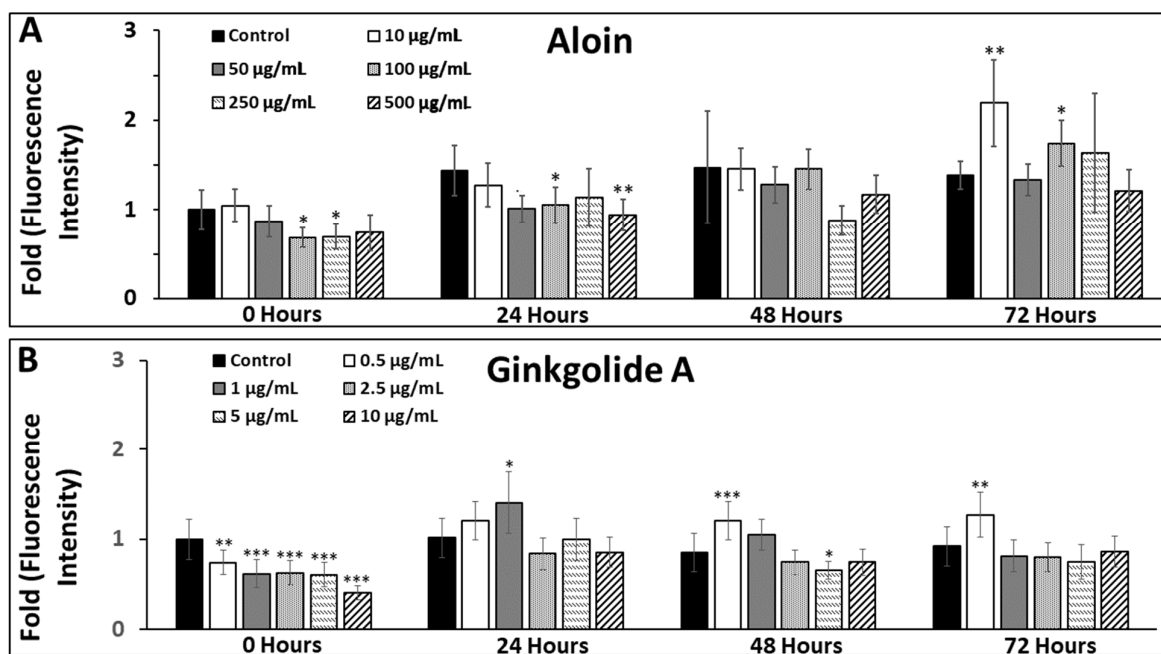


Figure 5. Changes in general oxidative stress (GOS) of Müller glia (MG) post-irradiation of 5-ion GCR in response to exogenous concentrations of aloin (A) and ginkgolide A (G). (A) GOS measured over time of MG cultured in control and titrated solutions of aloin 50 µg/mL and 100 µg/mL (suspended in DMEM). (B) GOS measured over time of MG cultured in control and titrated solutions of ginkgolide A 1 µg/mL and 2.5 µg/mL (suspended in DMEM). All values of GOS are normalized to control conditions (DMEM only). Statistical significance of $p < 0.05$ is denoted with an asterisk (*), and $p < 0.001$ is represented by a triple asterisk (**). Representative image of GOS expression in MG after 6 h post irradiation for (C) aloin control and (D) aloin 100 µg/mL. Scale bar = 50 µm.

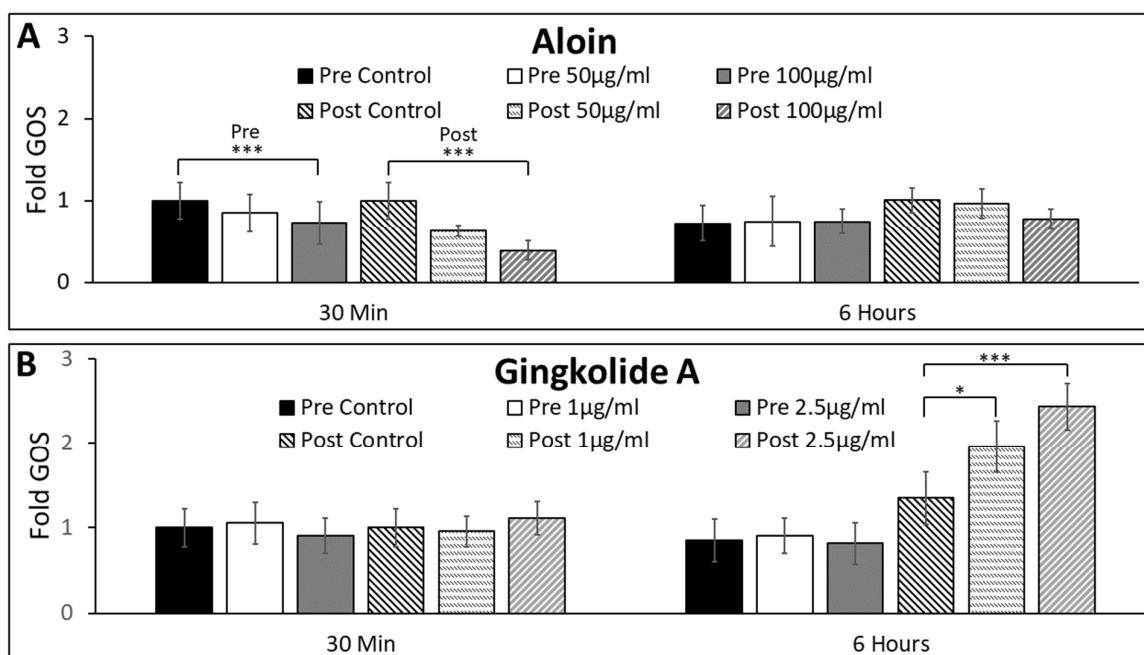


Figure 6. Changes in general oxidative stress (GOS) of Müller glia (MG) over time in response to exogenous concentrations of aloin (A) and ginkgolide A (G). Changes in the general oxidative stress (GOS) of Müller glia (MG) cells were measured when cultured with different concentrations of the antioxidants, aloin and ginkgolide A. (A) GOS measured over time of MG cultured in titrated solutions of 10, 50, 100, 250, and 500 µg/mL of aloin (suspended in DMEM). All values of GOS are normalized to control conditions (DMEM only). (B) GOS measured over time of MG cultured in titrated solutions of 0.5, 1, 2.5, 5, and 10 µg/mL ginkgolide A (suspended in DMEM). All values of GOS are normalized to control conditions (DMEM only). Statistical significance of $p < 0.05$ is denoted with an asterisk (*), $p < 0.01$ is denoted with a double asterisk (**), and $p < 0.001$ is represented by a triple asterisk (***)�. Scale bar = 50 µm.

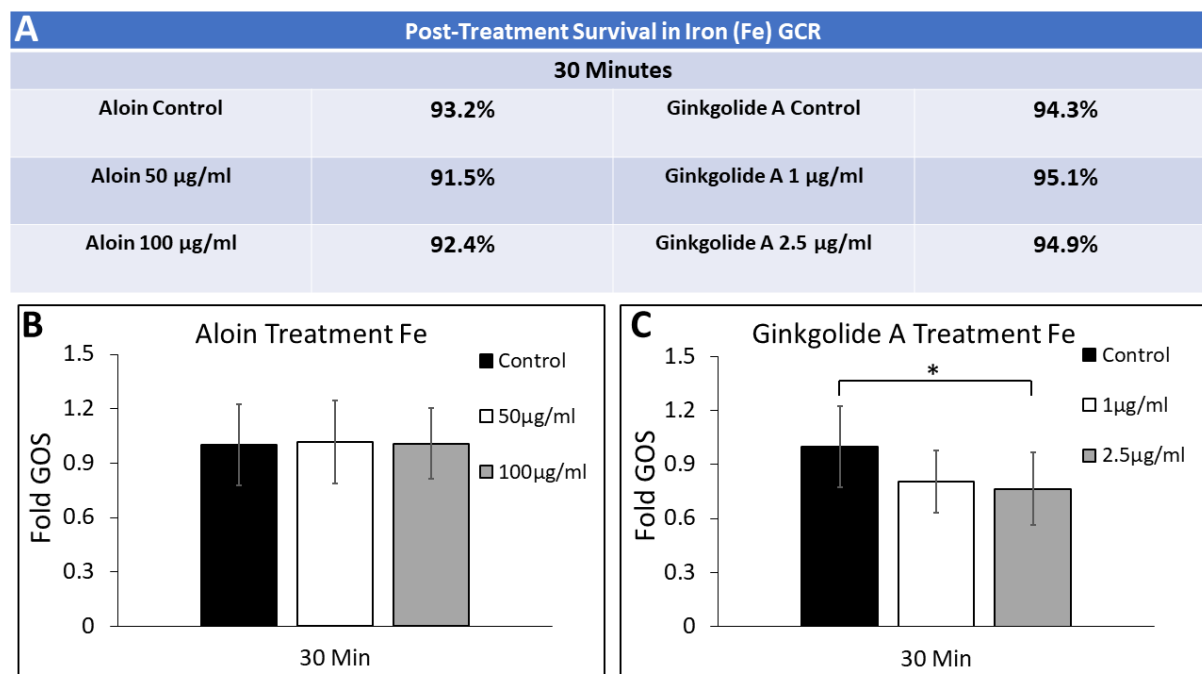


Figure 7. Changes in general oxidative stress (GOS) of Müller glia (MG) post-irradiation of iron GCR in response to exogenous concentrations of aloin (A) and ginkgolide A (G). (A) Survival rates of Müller

glia (MG) measured when cultured in different antioxidant solutions of aloin (A) and ginkgolide A (G) for 30 min post irradiation with iron. (B) GOS measured over time of MG cultured in control and titrated solutions of aloin 50 µg/mL and 100 µg/mL (suspended in DMEM). (C) GOS measured over time of MG cultured in control and titrated solutions of ginkgolide A 1 µg/mL and 2.5 µg/mL (suspended in DMEM). All values of GOS are normalized to control conditions (DMEM only). Statistical significance of $p < 0.05$ is denoted with an asterisk (*).

4. Discussion

Müller glia (MG) are critical cells that regulate the synapse of retinal neurons [52], support retinal-tissue structure and integrity [43,53], and initiate endogenous repair responses to injury and/or disease [54]. Within the retina, MG perform many of the functions entrusted to other neuroglia across the nervous system, such as the neuronal homeostasis supported by astrocytes and oligodendrocytes [55], regulation of extracellular fluid performed by ependymal cells [56], and the reparative morphology and motility responses of Schwann cells [48]. Significantly, MG additionally regulate metabolic activities that control retinal redox and glutamatergic homeostasis [57,58]. Redox reactions are essential to retinal health and function but produce elevated levels of reactive-oxygen species (ROS) that can lead to degenerated adult retina when accumulated over time (reviewed in [59]), particularly significant for degenerative diseases caused by aging as well as SANS.

Prolonged light exposure leads to the high metabolic and oxidative phosphorylation rate of retinal tissue, which is a principal source of ROS generated in the mitochondria of healthy retinal neurons [27,60,61]. The complex phototransduction processes needed for vision, therefore, require significant retinal-antioxidant protection (reviewed in [62]). Surprisingly, much of the literature related to oxidative stress in the retina has understated the important antioxidant roles of MG and instead focused on MG production of oxidative products with detrimental effects on retinal neurons, such as nitric oxide synthase [62]. While MG can certainly contribute to oxidative stress via dysfunction of glutamate uptake and glutathione synthesis, MG metabolic functions also provide potent antioxidant factors that prevent neural damage from oxidative stress. ROS generation has been recently linked to physiological signaling and protective mechanisms in retinal MG that regulates the phosphorylation of ERK1/2 (pERK1/2) during gliosis [63].

This study introduced exogenous antioxidants derived from natural products (NPs) to examine changes in ROS production within reactive MG. Well-studied NP antioxidants were used to examine MG responses given the meteoric rise of nutraceuticals and dietary-supplement markets in recent decades [23]. The therapeutic benefits of aloin and ginkgo extracts have a long-standing history of use in traditional and holistic medicine [64,65], while more recent experimental and clinical studies have illustrated their potential neuroprotective benefits in a wide range of pathologies [66–68]. Specifically, biomedical experiments have demonstrated that aloin can inhibit retinal inflammation [39] and ginkgolide A can protect retinal tissue from oxidative stress [69].

Tests of the current study illustrated that extracellular solutions of the selected antioxidants led to significant decreases in the ROS of MG, over time, in culture. Most prevalently, (Figures 3A and 4A), the use of aloin and ginkgolide A produced an immediate decrease in ROS across MG cells. We have shown in Table 1 and Figure 6 that there are no adverse effects of the antioxidants on cultured glia. This baseline allowed us to examine how the antioxidants aid recovery of glia exposed to radiative damage. However, this decrease was abated, as MG levels of ROS returned to those of the control with extended time. The statistically significant increases in ROS levels of cultured MG suggests a dosage dependency that may be related to intracellular signaling pathways. Studies have found that the suppression of ROS stimulated by a more antioxidant-filled environment may induce homeostatic changes through the production of ROS-producing organelles [70]. By further increasing the antioxidant concentration, we may disrupt homeostatic equilibrium in the culture. For example, MG illustrated significantly elongated morphology at 72 h within the A-3 treatment group, as seen in Figure 3A (aloin, 100 µg/mL). It is believed that the

introduction of this antioxidant at this concentration may reveal a more *in vivo* morphology of the MG cells, characterized by further elongation of processes, which decreases to the size of the cell body [39].

Spaceflight-associated neuro-ocular syndrome (SANS) is a difficult syndrome to study, as it describes a series of pathologies observed primarily in prolonged spaceflight that uniquely impacts the aerospace community (reviewed in [1]). Although the contribution of radiation to SANS pathologies is incompletely examined, the impacts of radiation on neuroglia, and the retina more broadly, remain understudied. Our results illustrate that aloin provided immediate reduction in reactive oxygen species (ROS) against low-dose radiation. In complement, ginkgolide A provided an ROS reduction immediately in cases of high-dose radiation. These results are among the first to examine treatment of radiation damage via natural products and demonstrate the merit for further application in SANS and potentially other degenerative retinal conditions.

In summary, results of our study illustrate that retinal cells can be examined within both natural-product solutions and radiative environments. The use of natural products for retinal-cell health against radiative damage illustrates radiation-dose dependence and antioxidant-dose dependence. Moreover, the roles of natural products and ionizing radiation in neurobiological problems is a prime consideration with the increasing prevalence of spaceflight and space tourism.

Supplementary Materials: The following supporting information can be downloaded at: <https://www.mdpi.com/article/10.3390/neuroglia3030006/s1>. Figure S1: Naming procedure used for aloin and ginkgolide A studies.

Author Contributions: Conceptualization, R.N.C., N.C., G.L., L.Q., H.v.d.M. and M.V.; Data curation, R.N.C. and N.C.; Formal analysis, R.N.C., N.C. and T.R.; Funding acquisition, G.L., L.Q. and H.v.d.M.; Investigation, M.V.; Methodology, R.N.C. and N.C.; Project administration, G.L., L.Q. and H.v.d.M.; Resources, T.R.; Supervision, T.R. and M.V.; Writing—original draft, R.N.C. and N.C.; Writing—review & editing, R.N.C., N.C. and M.V. All authors have read and agreed to the published version of the manuscript.

Funding: This research was funded by Dr. Greg Olson and grant numbers (NJSGC# 80NSSC20M0066) and (CBET#180441, EEC-19-50509) and the APC was funded by (CBET#180441, EEC-19-50509).

Institutional Review Board Statement: Not applicable.

Informed Consent Statement: Not applicable.

Acknowledgments: This work was supported by the National Science Foundation (CBET#180441, EEC-19-50509) and the New Jersey Space Grant Consortium Fellowship (NJSGC# 80NSSC20M0066). The authors thank Juan S. Peña for their research contributions and development of Figure 1. The authors would also like to thank Greg Olsen for their generous financial support of this research.

Conflicts of Interest: The authors declare no conflict of interest.

References

- Martin Paez, Y.; Mudie, L.I.; Subramanian, P.S. Spaceflight Associated Neuro-Ocular Syndrome (SANS): A Systematic Review and Future Directions. *Eye Brain* **2020**, *12*, 105–117. [[CrossRef](#)] [[PubMed](#)]
- Mao, X.W.; Boerma, M.; Rodriguez, D.; Campbell-Beachler, M.; Jones, T.; Stanbouly, S.; Sridharan, V.; Nishiyama, N.C.; Wroe, A.; Nelson, G.A. Combined Effects of Low-Dose Proton Radiation and Simulated Microgravity on the Mouse Retina and the Hematopoietic System. *Radiat. Res.* **2019**, *192*, 241–250. [[CrossRef](#)] [[PubMed](#)]
- Mao, X.W.; Boerma, M.; Rodriguez, D.; Campbell-Beachler, M.; Jones, T.; Stanbouly, S.; Sridharan, V.; Wroe, A.; Nelson, G.A. Acute Effect of Low-Dose Space Radiation on Mouse Retina and Retinal Endothelial Cells. *Radiat. Res.* **2018**, *190*, 45–52. [[CrossRef](#)]
- Lett, J.T.; Cox, A.B.; Bergtold, D.S. Cellular and tissue responses to heavy ions: Basic considerations. *Radiat. Environ. Biophys.* **1986**, *25*, 1–12. [[CrossRef](#)] [[PubMed](#)]
- Loganovsky, K.N.; Marazziti, D.; Fedirko, P.A.; Kuts, K.V.; Antypchuk, K.Y.; Perchuk, I.V.; Babenko, T.F.; Loganovska, T.K.; Kolosynska, O.O.; Kreinis, G.Y.; et al. Radiation-Induced Cerebro-Ophthalmic Effects in Humans. *Life* **2020**, *10*, 41. [[CrossRef](#)]
- Vazquez, M.E.; Kirk, E. In vitro neurotoxic effects of 1 GeV/n iron particles assessed in retinal explants. *Adv. Space Res.* **2000**, *25*, 2041–2049. [[CrossRef](#)]

7. Williams, G.R.; Lett, J.T. Damage to the photoreceptor cells of the rabbit retina from 56Fe ions: Effect of age at exposure, 1. *Adv. Space Res.* **1996**, *18*, 55–58. [[CrossRef](#)]
8. Krebs, W.; Krebs, I.; Worgul, B.V. Effect of accelerated iron ions on the retina. *Radiat. Res.* **1990**, *123*, 213–219. [[CrossRef](#)]
9. Nelson, A.C.; Hayes, T.L.; Tobias, C.A.; Yang, T.C. Some indications of structural damage in retina by heavy ion radiation. *Scan. Electron. Microsc.* **1981**, *4*, 79–85.
10. Mohler, S.R. Galactic radiation exposure during commercial flights: Is there a risk? *CMAJ* **2003**, *168*, 1157–1158.
11. Lerner, D.J.; Gorog, J.M., Jr. How “Rad” Is a Trip to Space? A Brief Discussion of Radiation Exposure in Suborbital Space Tourism. *J. Am. Coll. Radiol.* **2021**, *18*, 225–228. [[CrossRef](#)] [[PubMed](#)]
12. Kiser, P.D.; Golczak, M.; Maeda, A.; Palczewski, K. Key enzymes of the retinoid (visual) cycle in vertebrate retina. *Biochim. Biophys. Acta* **2012**, *1821*, 137–151. [[CrossRef](#)] [[PubMed](#)]
13. Leveillard, T.; Sahel, J.A. Metabolic and redox signaling in the retina. *Cell Mol. Life Sci.* **2017**, *74*, 3649–3665. [[CrossRef](#)] [[PubMed](#)]
14. Nita, M.; Grzybowski, A. The Role of the Reactive Oxygen Species and Oxidative Stress in the Pathomechanism of the Age-Related Ocular Diseases and Other Pathologies of the Anterior and Posterior Eye Segments in Adults. *Oxid. Med. Cell Longev.* **2016**, *2016*, 3164734. [[CrossRef](#)]
15. Upadhyay, M.; Milliner, C.; Bell, B.A.; Bonilha, V.L. Oxidative stress in the retina and retinal pigment epithelium (RPE): Role of aging, and DJ-1. *Redox Biol.* **2020**, *37*, 101623. [[CrossRef](#)] [[PubMed](#)]
16. Ruan, Y.; Jiang, S.; Musayeva, A.; Gericke, A. Oxidative Stress and Vascular Dysfunction in the Retina: Therapeutic Strategies. *Antioxidants* **2020**, *9*, 761. [[CrossRef](#)]
17. Redza-Dutordoir, M.; Averill-Bates, D.A. Activation of apoptosis signalling pathways by reactive oxygen species. *Biochim. Biophys. Acta* **2016**, *1863*, 2977–2992. [[CrossRef](#)]
18. Bellezza, I. Oxidative Stress in Age-Related Macular Degeneration: Nrf2 as Therapeutic Target. *Front. Pharmacol.* **2018**, *9*, 1280. [[CrossRef](#)]
19. Calderon, G.D.; Juarez, O.H.; Hernandez, G.E.; Punzo, S.M.; de la Cruz, Z.D. Oxidative stress and diabetic retinopathy: Development and treatment. *Eye* **2017**, *31*, 1122–1130. [[CrossRef](#)]
20. Murakami, Y.; Nakabeppe, Y.; Sonoda, K.H. Oxidative Stress and Microglial Response in Retinitis Pigmentosa. *Int. J. Mol. Sci.* **2020**, *21*, 7170. [[CrossRef](#)]
21. Chauhan, B.; Kumar, G.; Kalam, N.; Ansari, S.H. Current concepts and prospects of herbal nutraceutical: A review. *J. Adv. Pharm. Technol. Res.* **2013**, *4*, 4–8. [[PubMed](#)]
22. Helal, N.A.; Eassa, H.A.; Amer, A.M.; Eltokhy, M.A.; Edafiogho, I.; Nounou, M.I. Nutraceuticals’ Novel Formulations: The Good, the Bad, the Unknown and Patents Involved. *Recent Pat. Drug Deliv. Formul.* **2019**, *13*, 105–156. [[CrossRef](#)] [[PubMed](#)]
23. Lordan, R. Dietary supplements and nutraceuticals market growth during the coronavirus pandemic—Implications for consumers and regulatory oversight. *Pharma Nutr.* **2021**, *18*, 100282. [[CrossRef](#)] [[PubMed](#)]
24. Nasri, H.; Baradaran, A.; Shirzad, H.; Rafieian-Kopaei, M. New concepts in nutraceuticals as alternative for pharmaceuticals. *Int. J. Prev. Med.* **2014**, *5*, 1487–1499. [[PubMed](#)]
25. Lobo, G.P.; Biswal, M.R.; Kondkar, A.A. Editorial: Molecular Mechanisms of Retinal Cell Degeneration and Regeneration. *Front. Cell Dev. Biol.* **2021**, *9*, 667028. [[CrossRef](#)]
26. Babizhayev, M.A.; Deyev, A.I.; Yermakova, V.N.; Brikman, I.V.; Bours, J. Lipid peroxidation and cataracts: N-acetylcarnosine as a therapeutic tool to manage age-related cataracts in human and in canine eyes. *Drugs R D* **2004**, *5*, 125–139. [[CrossRef](#)]
27. Rohowitz, L.J.; Kraus, J.G.; Koulen, P. Reactive Oxygen Species-Mediated Damage of Retinal Neurons: Drug Development Targets for Therapies of Chronic Neurodegeneration of the Retina. *Int. J. Mol. Sci.* **2018**, *19*, 3362. [[CrossRef](#)]
28. Sanhueza Salas, L.F.; Garcia-Venzor, A.; Beltramone, N.; Capurro, C.; Toiber, D.; Silberman, D.M. Metabolic Imbalance Effect on Retinal Muller Glial Cells Reprogramming Capacity: Involvement of Histone Deacetylase SIRT6. *Front. Genet.* **2021**, *12*, 769723. [[CrossRef](#)]
29. Wang, J.; O’Sullivan, M.L.; Mukherjee, D.; Punal, V.M.; Farsiu, S.; Kay, J.N. Anatomy and spatial organization of Muller glia in mouse retina. *J. Comp. Neurol.* **2017**, *525*, 1759–1777. [[CrossRef](#)]
30. Kumar, A.; Pandey, R.K.; Miller, L.J.; Singh, P.K.; Kanwar, M. Muller glia in retinal innate immunity: A perspective on their roles in endophthalmitis. *Crit. Rev. Immunol.* **2013**, *33*, 119–135. [[CrossRef](#)]
31. Hippert, C.; Graca, A.B.; Barber, A.C.; West, E.L.; Smith, A.J.; Ali, R.R.; Pearson, R.A. Muller glia activation in response to inherited retinal degeneration is highly varied and disease-specific. *PLoS ONE* **2015**, *10*, e0120415. [[CrossRef](#)] [[PubMed](#)]
32. Graca, A.B.; Hippert, C.; Pearson, R.A. Muller Glia Reactivity and Development of Gliosis in Response to Pathological Conditions. *Adv. Exp. Med. Biol.* **2018**, *1074*, 303–308. [[PubMed](#)]
33. Bringmann, A.; Wiedemann, P. Muller glial cells in retinal disease. *Ophthalmologica* **2012**, *227*, 1–19. [[CrossRef](#)] [[PubMed](#)]
34. Nelson, C.M.; Ackerman, K.M.; O’Hayer, P.; Bailey, T.J.; Gorsuch, R.A.; Hyde, D.R. Tumor necrosis factor-alpha is produced by dying retinal neurons and is required for Muller glia proliferation during zebrafish retinal regeneration. *J. Neurosci.* **2013**, *33*, 6524–6539. [[CrossRef](#)]
35. Jiang, G.; Mysona, B.; Dun, Y.; Gnana-Prakasam, J.P.; Pabla, N.; Li, W.; Dong, Z.; Ganapathy, V.; Smith, S.B. Expression, subcellular localization, and regulation of sigma receptor in retinal muller cells. *Invest. Ophthalmol. Vis. Sci.* **2006**, *47*, 5576–5582. [[CrossRef](#)]
36. Bringmann, A.; Grosche, A.; Pannicke, T.; Reichenbach, A. GABA and Glutamate Uptake and Metabolism in Retinal Glial (Muller) Cells. *Front. Endocrinol.* **2013**, *4*, 48. [[CrossRef](#)]

37. Kay, A.M.; Simpson, C.L.; Stewart, J.A., Jr. The Role of AGE/RAGE Signaling in Diabetes-Mediated Vascular Calcification. *J. Diabetes Res.* **2016**, *2016*, 6809703. [[CrossRef](#)]
38. Dorrell, M.I.; Aguilar, E.; Jacobson, R.; Yanes, O.; Gariano, R.; Heckenlively, J.; Banin, E.; Ramirez, G.A.; Gasmi, M.; Bird, A.; et al. Antioxidant or neurotrophic factor treatment preserves function in a mouse model of neovascularization-associated oxidative stress. *J. Clin. Investig.* **2009**, *119*, 611–623. [[CrossRef](#)]
39. Jung, E.; Kim, J. Aloin Inhibits Muller Cells Swelling in a Rat Model of Thioacetamide-Induced Hepatic Retinopathy. *Molecules* **2018**, *23*, 2806. [[CrossRef](#)]
40. Liu, Q.; Jin, Z.; Xu, Z.; Yang, H.; Li, L.; Li, G.; Li, F.; Gu, S.; Zong, S.; Zhou, J.; et al. Antioxidant effects of ginkgolides and bilobalide against cerebral ischemia injury by activating the Akt/Nrf2 pathway in vitro and in vivo. *Cell Stress Chaperones* **2019**, *24*, 441–452. [[CrossRef](#)]
41. Walchuk, C.; Suh, M. Nutrition and the aging retina: A comprehensive review of the relationship between nutrients and their role in age-related macular degeneration and retina disease prevention. *Adv. Food Nutr. Res.* **2020**, *93*, 293–332. [[PubMed](#)]
42. Labkovich, M.; Jacobs, E.B.; Bhargava, S.; Pasquale, L.R.; Ritch, R. Ginkgo Biloba Extract in Ophthalmic and Systemic Disease, With a Focus on Normal-Tension Glaucoma. *Asia Pac. J. Ophthalmol.* **2020**, *9*, 215–225. [[CrossRef](#)] [[PubMed](#)]
43. Wang, Z.Y.; Mo, X.F.; Jiang, X.H.; Rong, X.F.; Miao, H.M. Ginkgolide B promotes axonal growth of retina ganglion cells by anti-apoptosis in vitro. *Sheng Li Xue Bao* **2012**, *64*, 417–424. [[PubMed](#)]
44. Sarthy, V.P.; Brodjian, S.J.; Dutt, K.; Kennedy, B.N.; French, R.P.; Crabb, J.W. Establishment and characterization of a retinal Muller cell line. *Invest. Ophthalmol. Vis. Sci.* **1998**, *39*, 212–216. [[PubMed](#)]
45. Pena, J.S.; Vazquez, M. VEGF Upregulates EGFR Expression to Stimulate Chemotactic Behaviors in the rMC-1 Model of Muller Glia. *Brain Sci.* **2020**, *10*, 330. [[CrossRef](#)]
46. Trueblood, K.E.; Mohr, S.; Dubyak, G.R. Purinergic regulation of high-glucose-induced caspase-1 activation in the rat retinal Muller cell line rMC-1. *Am. J. Physiol. Cell Physiol.* **2011**, *301*, C1213–C1223. [[CrossRef](#)]
47. Xue, W.; Du, P.; Lin, S.; Dudley, V.J.; Hernandez, M.R.; Sarthy, V.P. Gene expression changes in retinal Muller (glial) cells exposed to elevated pressure. *Curr. Eye Res.* **2011**, *36*, 754–767. [[CrossRef](#)]
48. Cliver, R.N.; Ayers, B.; Brady, A.; Firestein, B.L.; Vazquez, M. Cerebrospinal fluid replacement solutions promote neuroglia migratory behaviors and spinal explant outgrowth in microfluidic culture. *J. Tissue Eng. Regen. Med.* **2021**, *15*, 176–188. [[CrossRef](#)]
49. Pena, J.; Dulger, N.; Singh, T.; Zhou, J.; Majeska, R.; Redenti, S.; Vazquez, M. Controlled microenvironments to evaluate chemotactic properties of cultured Muller glia. *Exp. Eye Res.* **2018**, *173*, 129–137. [[CrossRef](#)]
50. Grosche, A.; Hauser, A.; Lepper, M.F.; Mayo, R.; von Toerne, C.; Merl-Pham, J.; Hauck, S.M. The Proteome of Native Adult Muller Glial Cells from Murine Retina. *Mol. Cell Proteom.* **2016**, *15*, 462–480. [[CrossRef](#)]
51. Norbury, J.W.; Schimmerling, W.; Slaba, T.C.; Azzam, E.I.; Badavi, F.F.; Baiocco, G.; Benton, E.; Bindi, V.; Blakely, E.A.; Blattnig, S.R.; et al. Galactic cosmic ray simulation at the NASA Space Radiation Laboratory. *Life Sci. Space Res.* **2016**, *8*, 38–51. [[CrossRef](#)] [[PubMed](#)]
52. Reichenbach, A.; Bringmann, A. Glia of the human retina. *Glia* **2020**, *68*, 768–796. [[CrossRef](#)] [[PubMed](#)]
53. Philips, T.; Rothstein, J.D. Oligodendroglia: Metabolic supporters of neurons. *J. Clin. Investig.* **2017**, *127*, 3271–3280. [[CrossRef](#)] [[PubMed](#)]
54. Goldman, D. Muller glial cell reprogramming and retina regeneration. *Nat. Rev. Neurosci.* **2014**, *15*, 431–442. [[CrossRef](#)] [[PubMed](#)]
55. Ricci, G.; Volpi, L.; Pasquali, L.; Petrozzi, L.; Siciliano, G. Astrocyte-neuron interactions in neurological disorders. *J. Biol. Phys.* **2009**, *35*, 317–336. [[CrossRef](#)] [[PubMed](#)]
56. Hladky, S.B.; Barrand, M.A. Mechanisms of fluid movement into, through and out of the brain: Evaluation of the evidence. *Fluids Barriers CNS* **2014**, *11*, 26. [[CrossRef](#)] [[PubMed](#)]
57. Ardourel, M.; Felgerolle, C.; Paris, A.; Acar, N.; Othman, K.R.B.; Ueda, N.; Rossignol, R.; Bazinet, A.; Hebert, B.; Briault, S.; et al. Dietary Supplement Enriched in Antioxidants and Omega-3 Promotes Glutamine Synthesis in Muller Cells: A Key Process against Oxidative Stress in Retina. *Nutrients* **2021**, *13*, 3216. [[CrossRef](#)]
58. Toft-Kehler, A.K.; Skytt, D.M.; Kolko, M. A Perspective on the Muller Cell-Neuron Metabolic Partnership in the Inner Retina. *Mol. Neurobiol.* **2018**, *55*, 5353–5361. [[CrossRef](#)]
59. Reichenbach, A.; Bringmann, A. New functions of Muller cells. *Glia* **2013**, *61*, 651–678. [[CrossRef](#)]
60. Kuse, Y.; Ogawa, K.; Tsuruma, K.; Shimazawa, M.; Hara, H. Damage of photoreceptor-derived cells in culture induced by light emitting diode-derived blue light. *Sci. Rep.* **2014**, *4*, 5223. [[CrossRef](#)]
61. Payne, A.J.; Kaja, S.; Naumchuk, Y.; Kunjukunju, N.; Koulen, P. Antioxidant drug therapy approaches for neuroprotection in chronic diseases of the retina. *Int. J. Mol. Sci.* **2014**, *15*, 1865–1886. [[CrossRef](#)] [[PubMed](#)]
62. Eastlake, K.; Luis, J.; Limb, G.A. Potential of Muller Glia for Retina Neuroprotection. *Curr. Eye Res.* **2020**, *45*, 339–348. [[CrossRef](#)] [[PubMed](#)]
63. Groeger, G.; Doonan, F.; Cotter, T.G.; Donovan, M. Reactive oxygen species regulate prosurvival ERK1/2 signaling and bFGF expression in gliosis within the retina. *Invest. Ophthalmol. Vis. Sci.* **2012**, *53*, 6645–6654. [[CrossRef](#)] [[PubMed](#)]
64. Chassagne, F.; Huang, X.; Lyles, J.T.; Quave, C.L. Validation of a 16th Century Traditional Chinese Medicine Use of Ginkgo biloba as a Topical Antimicrobial. *Front. Microbiol.* **2019**, *10*, 775. [[CrossRef](#)] [[PubMed](#)]

65. Chassagne, F.; Samarakoon, T.; Porras, G.; Lyles, J.T.; Dettweiler, M.; Marquez, L.; Salam, A.M.; Shabih, S.; Farrokhi, D.R.; Quave, C.L. A Systematic Review of Plants with Antibacterial Activities: A Taxonomic and Phylogenetic Perspective. *Front. Pharmacol.* **2020**, *11*, 586548. [[CrossRef](#)]
66. Bosch-Morell, F.; Villagrasa, V.; Ortega, T.; Acero, N.; Munoz-Mingarro, D.; Gonzalez-Rosende, M.E.; Castillo, E.; Sanahuja, M.A.; Soriano, P.; Martinez-Solis, I. Medicinal plants and natural products as neuroprotective agents in age-related macular degeneration. *Neural Regen. Res.* **2020**, *15*, 2207–2216.
67. Mojaverrostami, S.; Bojnordi, M.N.; Ghasemi-Kasman, M.; Ebrahimzadeh, M.A.; Hamidabadi, H.G. A Review of Herbal Therapy in Multiple Sclerosis. *Adv. Pharm. Bull.* **2018**, *8*, 575–590. [[CrossRef](#)]
68. Tewari, D.; Samoila, O.; Gocan, D.; Mocan, A.; Moldovan, C.; Devkota, H.P.; Atanasov, A.G.; Zengin, G.; Echeverria, J.; Vodnar, D.; et al. Medicinal Plants and Natural Products Used in Cataract Management. *Front. Pharmacol.* **2019**, *10*, 466. [[CrossRef](#)]
69. Zhou, Y.Y.; Chen, C.Z.; Su, Y.; Li, L.; Yi, Z.H.; Qi, H.; Weng, M.; Xing, Y.Q. Effect of EGb761 on light-damaged retinal pigment epithelial cells. *Int. J. Ophthalmol.* **2014**, *7*, 8–13.
70. St-Pierre, J.; Drori, S.; Uldry, M.; Silvaggi, J.M.; Rhee, J.; Jager, S.; Handschin, C.; Zheng, K.; Lin, J.; Yang, W.; et al. Suppression of reactive oxygen species and neurodegeneration by the PGC-1 transcriptional coactivators. *Cell* **2006**, *127*, 397–408. [[CrossRef](#)]